

UC Santa Cruz

UC Santa Cruz Previously Published Works

Title

Stable Occupancy of the Crimean-Congo Hemorrhagic Fever Virus-Encoded Deubiquitinase Blocks Viral Infection.

Permalink

<https://escholarship.org/uc/item/9fq1j0tm>

Journal

mBio, 10(4)

Authors

Scholte, Florine

Hua, Brian

Spengler, Jessica

et al.

Publication Date

2019-07-23







DOI

10.1128/mBio.01065-19

Peer reviewed



Stable Occupancy of the Crimean-Congo Hemorrhagic Fever Virus-Encoded Deubiquitinase Blocks Viral Infection

 Florine E. M. Scholte,^a  Brian L. Hua,^a  Jessica R. Spengler,^a John V. Dzimianski,^b JoAnn D. Coleman-McCray,^a  Stephen R. Welch,^a  Laura K. McMullan,^a Stuart T. Nichol,^a Scott D. Pegan,^b Christina F. Spiropoulou,^a  Éric Bergeron^a

^aViral Special Pathogens Branch, Division of High-Consequence Pathogens and Pathology, National Center for Emerging and Zoonotic Infectious Diseases, Centers for Disease Control and Prevention, Atlanta, Georgia, USA

^bDepartment of Pharmaceutical and Biomedical Sciences, University of Georgia, Athens, Georgia, USA

ABSTRACT Crimean-Congo hemorrhagic fever virus (CCHFV) infection can result in a severe hemorrhagic syndrome for which there are no antiviral interventions available to date. Certain RNA viruses, such as CCHFV, encode cysteine proteases of the ovarian tumor (OTU) family that antagonize interferon (IFN) production by deconjugating ubiquitin (Ub). The OTU of CCHFV, a negative-strand RNA virus, is dispensable for replication of the viral genome, despite being part of the large viral RNA polymerase. Here, we show that mutations that prevent binding of the OTU to cellular ubiquitin are required for the generation of recombinant CCHFV containing a mutated catalytic cysteine. Similarly, the high-affinity binding of a synthetic ubiquitin variant (UbV-CC4) to CCHFV OTU strongly inhibits viral growth. UbV-CC4 inhibits CCHFV infection even in the absence of intact IFN signaling, suggesting that its antiviral activity is not due to blocking the OTU's immunosuppressive function. Instead, the prolonged occupancy of the OTU with UbV-CC4 directly targets viral replication by interfering with CCHFV RNA synthesis. Together, our data provide mechanistic details supporting the development of antivirals targeting viral OTUs.

IMPORTANCE Crimean-Congo hemorrhagic fever virus is an important human pathogen with a wide global distribution for which no therapeutic interventions are available. CCHFV encodes a cysteine protease belonging to the ovarian tumor (OTU) family which is involved in host immune suppression. Here we demonstrate that artificially prolonged binding of the OTU to a substrate inhibits virus infection. This provides novel insights into CCHFV OTU function during the viral replicative cycle and highlights the OTU as a potential antiviral target.

KEYWORDS *Nairoviridae*, RNA replication, antiviral agents, bunyavirus, innate immunity, interferon-stimulated gene-15, proteases, ubiquitination

Crimean-Congo hemorrhagic fever virus (CCHFV; family *Nairoviridae*) can cause mild disease or progress to a severe hemorrhagic syndrome associated with high morbidity and mortality. CCHF is the most widespread tick-borne viral disease affecting humans, and cases have been reported in Europe, Asia, the Middle East, and Africa. Serological evidence indicates infection of numerous mammalian species, including wild animals and livestock (e.g., cattle, sheep, and goats) (1). While infected vertebrates are generally asymptomatic, they serve a key role in the maintenance and transmission cycle of the virus as amplifying hosts for the tick reservoir and vector. CCHFV's main reservoir and vector are ticks of the *Hyalomma* genus, which are widely distributed throughout large portions of Europe, Africa, the Middle East, and Asia, and these current ecological niches are likely expanding (2, 3). The first identification of CCHF cases in Spain in 2016 illustrates how the virus might spread from areas of endemicity

Citation Scholte FEM, Hua BL, Spengler JR, Dzimianski JV, Coleman-McCray JD, Welch SR, McMullan LK, Nichol ST, Pegan SD, Spiropoulou CF, Bergeron É. 2019. Stable occupancy of the Crimean-Congo hemorrhagic fever virus-encoded deubiquitinase blocks viral infection. *mBio* 10:e01065-19. <https://doi.org/10.1128/mBio.01065-19>.

Editor Cristina Risco Ortiz, Centro Nacional de Biotecnología

This is a work of the U.S. Government and is not subject to copyright protection in the United States. Foreign copyrights may apply. Address correspondence to Éric Bergeron, ebergeron@cdc.gov.

B.L.H. and J.R.S. contributed equally to this article.

Received 29 April 2019

Accepted 25 June 2019

Published 23 July 2019

to Western Europe with the assistance of migratory birds carrying infected ticks over long distances (4, 5).

CCHF case-fatality rates typically range from 5% to 40% (6). Nosocomial transmission is common before patient isolation and strict nursing barriers are implemented. These nosocomial outbreaks are aided by the fact that CCHF initially manifests as a nonspecific febrile illness, thereby increasing its potential to initiate chains of human transmission. Although ribavirin has been used to treat CCHF, its efficacy and utility in clinical settings remain under debate, and no licensed vaccines or alternative therapeutic options are available to prevent disease or treat patients. Therefore, novel antiviral strategies are required to combat outbreaks.

CCHFV possesses a negative-strand trisegmented RNA genome. The small (S) segment encodes the nucleoprotein (NP), the medium (M) segment encodes the glycoprotein precursor (GPC), and the large (L) segment encodes the multifunctional L protein that contains the RNA-dependent RNA polymerase (RdRp) and an ovarian tumor (OTU)-like cysteine protease domain. The CCHFV OTU domain possesses deubiquitinase (DUB) and deISGylase activity, enabling the removal of ubiquitin (Ub) and ubiquitin-like interferon (IFN)-stimulated gene 15 (ISG15) conjugates from their protein targets (7–9). Ub and ISG15 are small proteins involved in regulating cellular signaling, including innate immune responses. Innate immune responses are activated when immune receptors detect pathogen-associated molecular patterns (PAMPs), triggering various downstream signaling pathways and resulting in the production of interferons and the activation or upregulation of antiviral effector proteins.

Protein ubiquitination is required for the expression of type I interferon (IFN), which upregulates hundreds of IFN-stimulated genes critical for rapidly restricting viral replication. Cellular deubiquitinases (DUBs) can dampen IFN responses by removing Ub from key proteins regulating immunity, including RIG-I, MAVS, TRAF3, TBK1, and IRF3 (10). Unsurprisingly, various virus families encode DUB domains. Viral DUBs belonging to the OTU superfamily have been reported for both positive-strand (*Tymoviridae* and *Arteriviridae*) and negative-strand (*Nairoviridae* and *Tenuivirus*) RNA viruses (7, 9, 11–17). Viral DUBs are thought to facilitate viral replication by modulating innate immune responses as well as by reducing Ub-mediated degradation of viral proteins by the proteasome. For example, viral DUB activity of CCHFV OTU and equine arteritis virus OTU suppresses type I IFN signaling during infection (7–9), whereas the turnip yellow mosaic virus DUB counters Ub-mediated proteasomal degradation of its polymerase (17). Study of the role of DUBs encoded by positive-strand RNA viruses is hindered by the fact that this protease is involved in viral polyprotein processing required for RdRp maturation, and therefore catalytically inactive mutants cannot be generated. In contrast, negative-strand RNA viruses such as CCHFV do not require DUB activity for their RdRp to function (18). Thus, the ability of CCHFV to remove Ub conjugates is not an absolute requirement for viral growth, although disruption was shown previously to result in enhanced cellular antiviral responses (8).

In addition to Ub, certain viral DUBs can also remove ISG15 conjugates from target proteins. Both Ub and ISG15 are conjugated to lysine (K) residues via a three-step enzymatic cascade, comprising a ubiquitin-activating enzyme (E1), a ubiquitin-conjugating enzyme (E2), and a ubiquitin ligase (E3). Ub is constitutively expressed, whereas expression of ISG15 and its conjugating enzymes requires IFN stimulation. Ub conjugation is mediated by hundreds of E3 ligases, whereas ISG15 conjugation relies mainly on one E3 ligase (HERC5) (19, 20). ISGylation appears to be largely restricted to newly synthesized proteins due to HERC5 ribosomal association, thus making ISGs and viral proteins central targets (19–21). ISGylation can exert antiviral activity by prolonging antiviral signaling (IRF3, STAT) (22, 23) or by interfering with the function of viral proteins. For example, ISGylation can interfere with oligomerization of viral proteins, which is important for the formation of viral particles and ribonucleoprotein (RNP) complexes (19, 24). Therefore, viral DUBs such as CCHFV OTU are expected to counter innate immune responses by removing Ub and ISG15 conjugates from their target proteins. This makes viral DUBs attractive potential therapeutic targets, as disrupting

their activity is expected to enhance immune responses upon infection and hinder viral growth.

Here, we generated a catalytic inactive mutant of a negative-strand RNA virus (CCHFV) to investigate the role of the OTU during infection. Notably, rescue of a catalytic inactive CCHFV required an additional mutation to alleviate the interactions of the OTU with cellular Ub (C40A/Q16R). This revealed that inactivation or inhibition of the OTU domain of CCHFV can block viral replication. Likewise, an engineered ubiquitin variant (UbV) specific for CCHFV OTU (UbV-CC4) also strongly inhibited CCHFV growth by hindering viral transcription and/or replication. Despite the reported immune suppression function of the OTU, this inhibition was largely independent of OTU-mediated IFN suppression. Therefore, prolonged binding of the OTU to Ub or a CCHFV OTU-specific inhibitor (CC4) blocked viral infection. These data support considering CCHFV OTU to be a prime target for future development of antiviral strategies, as such binding negates the immunosuppression mediated by the OTU and directly inhibits viral transcription and/or replication.

RESULTS

Disruption of OTU binding to Ub permits rescue of recombinant CCHFV containing a catalytically inactive OTU. Viral DUBs are thought to facilitate viral infection by manipulating host immune responses, but their exact mode of action remains elusive. We previously reported efficient recovery of DUB-deficient CCHFV when Q16 and A129, critical residues involved in Ub binding, were mutated (8). In contrast, previous attempts to rescue virus containing a mutated OTU catalytically active site (C40A) failed. Unexpectedly, a later attempt to generate a recombinant virus with the OTU-C40A mutation was successful. Sequencing the complete viral genome confirmed the conservation of the C40A mutation and revealed the acquisition of a nonconservative change at position 16 of the OTU (Q16P), indicating that Q16P may serve as an adaptive mutation allowing rescue of CCHFV encoding an inactive OTU. Strikingly, Q16 is a critical residue required for Ub binding (8, 25), suggesting that Ub binding to the inactive OTU prevents CCHFV rescue. To examine if disruption of Ub binding is critical for the rescue of the CCHFV-C40A mutant, we added the Q16R mutation to disrupt Ub binding to the OTU of the L-C40A mutant. Indeed, combining the C40A and Q16R mutations resulted in efficient recovery of recombinant CCHFV (Fig. 1a). Sequence analysis of a subsequent passage confirmed the presence of the C40A/Q16R mutations without any additional changes in the viral genome.

Next, we examined the effect of disrupting OTU catalytic activity on viral growth in A549 and BSR-T7/5 cells (Fig. 1b and c). Growth kinetics were assessed using CCHFV-ZsG reporter viruses by measuring ZsGreen1 (ZsG) fluorescence as an indicator of viral infection (26). Although a minor reduction in ZsG fluorescence was observed for CCHFV-C40A/Q16R, both the Q16R and C40A/Q16R OTU mutants grew efficiently in BSR-T7/5 cells, which are unable to mount an IFN response during infection (27). In contrast, growth of CCHFV-C40A/Q16R was severely impaired in A549 cells, which do mount a robust immune response during CCHFV infection (8). To confirm that the reduced growth kinetics of both mutant viruses in A549 cells was due to cellular immune responses, we assessed the growth kinetics of these viruses in A549 cells lacking RIG-I (RIG-I KO [knockout]) (Fig. 1d) and found that both CCHFV-Q16R and CCHFV-C40A/Q16R displayed enhanced growth kinetics in the absence of RIG-I signaling. This suggests that OTU activity is not an absolute requirement for CCHFV infection and specifically supports viral growth in IFN-competent cells.

OTU activity is not required for CCHFV lethality in IFNAR^{-/-} mice. Assessing the role of the OTU in CCHFV pathogenesis *in vivo* is limited by the fact that only type I IFN-deficient small-animal models (IFNAR^{-/-} and STAT1^{-/-} mice) are available. While the use of immunocompromised mice presents limitations in addressing the immune suppression function of the OTU, this model can nonetheless provide insights into the effects of altered OTU activity on CCHFV disease progression. To examine the effect of OTU mutations on disease, we infected IFNAR^{-/-} mice subcutaneously (1×10^2 50%

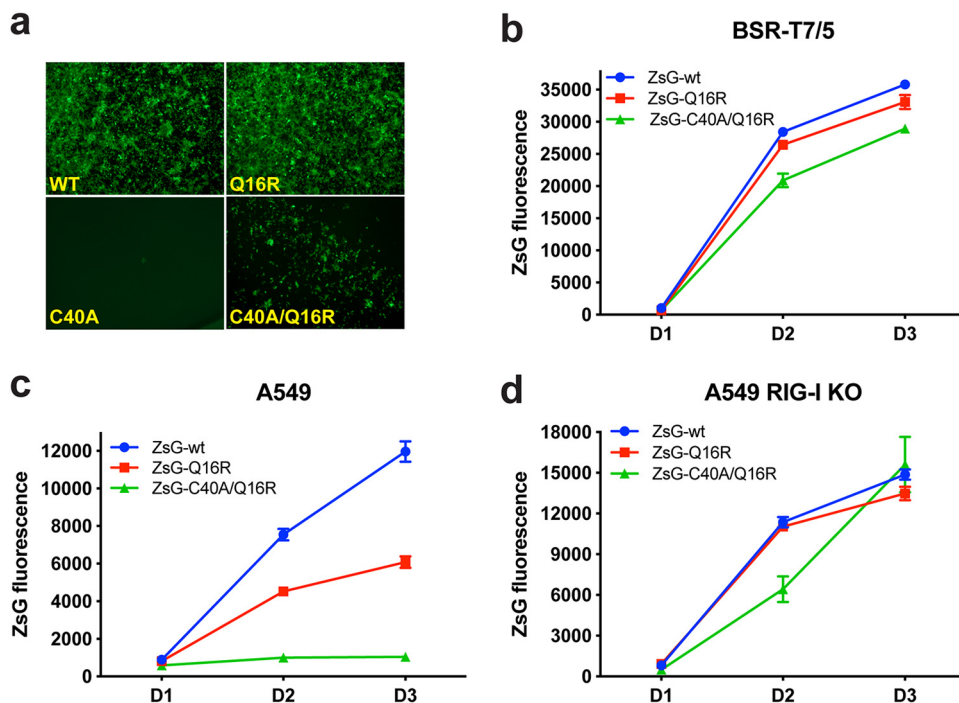


FIG 1 Generation of recombinant CCHFV containing an inactive OTU. (a) Recovery of ZsG-encoding CCHFV reporter viruses containing OTU mutations. Huh7 cells were transfected with plasmids encoding the full-length S, M, and L genome segments and with helper plasmids encoding NP, codon-optimized L, and T7 RNA polymerase. After 5 days, supernatants were transferred to fresh Huh7 cells, and ZsG fluorescence was imaged to determine successful virus rescue. WT, wild type. (b to d) Growth kinetics of recombinant CCHFV-ZsG viruses containing the indicated OTU mutations in A549, BSR-T7/5, and A549 RIG-I KO cells (multiplicity of infection [MOI] of 0.1). At the indicated time points (days [D]), ZsG fluorescence was quantified as a measure of viral replication. Data are presented as means \pm standard deviations (SD) of results from three replicates.

tissue culture infective doses [TCID₅₀]) and monitored weight and health daily (Fig. 2). All mice started losing weight 3 days after infection. Infection performed with CCHFV-Q16R, in which only Ub binding was disrupted, resulted in illness identical to that caused by wild-type CCHFV (CCHFV-wt); mice succumbed to disease at 4 to 5 days postinfection (dpi), and no clinical differences between these two groups were observed (Fig. 2a and b). Mice infected with CCHFV-C40A/Q16R lost weight at a slightly lower rate and had a prolonged time to death (6 to 7 dpi); 2 of the 8 animals survived infection. Analysis of viral RNA in various tissues at the time of death or euthanasia demonstrated similar viral loads between all the groups, with the exception of the 2 survivors, in which CCHFV RNA levels were markedly lower (Fig. 2c). Together, these data demonstrate that OTU catalytic activity is not required for pathogenesis in mice in the absence of type I IFN signaling, although mutating the catalytic site resulted in mild attenuation *in vivo* in comparison to active OTUs (wt and Q16R).

UbV-CC4 blocks OTU activity. OTUs of positive-strand RNA viruses are involved in proteolytic processing of viral proteins required for polymerase maturation and are therefore indispensable for replication. In contrast, OTUs of negative-strand RNA viruses, like CCHFV, are not essential for RNA polymerase activity (18). However, our data suggest that inactivating the catalytic site of CCHFV OTU also interferes with viral transcription and/or replication, due to its interaction with cellular Ub (Fig. 1). As a result of its inability to cleave substrates, OTU-C40A may display prolonged binding to ubiquitinated substrates, potentially affecting L protein stability or function and ultimately preventing viral growth. We rationalized that blocking the OTU catalytic site of CCHFV-wt using an inhibitor could impede viral infection in a similar fashion.

A synthetic Ub variant (UbV) that binds the CCHFV OTU with high levels of affinity and specificity *in vitro* was recently described (UbV-CC4) (28). UbV-CC4 resembles

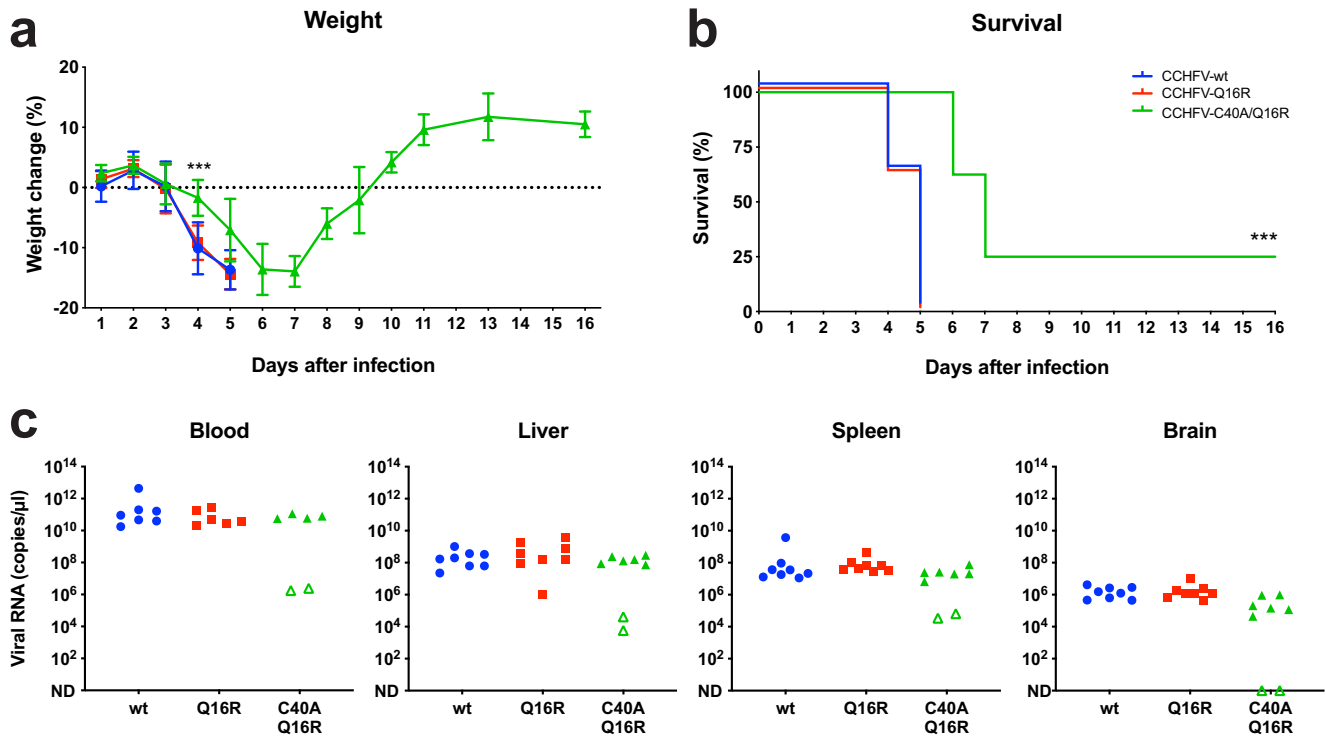


FIG 2 Lethality of CCHFV OTU mutants in an IFNAR^{-/-} mouse model. Female IFNAR^{-/-} mice (6 weeks of age) were infected subcutaneously with 100 TCID₅₀ of recombinant CCHFV (8 mice per group) and analyzed for weight (a) and survival (b). Animals were monitored daily for clinical signs of illness. Animal weights are shown as means ± SD and represent percentages of weight changes relative to a baseline set at 1 day before challenge. (c) The presence of viral RNA in blood and various homogenized tissues was analyzed using quantitative RT-PCR. The two survivors are indicated with open symbols. ***, statistical significance ($P < 0.001$) of results of comparisons between CCHFV-wt and CCHFV-C40A/Q16R.

cellular Ub, but the consensus LRLRGG motif required for cleavage and conjugation of Ub to proteins is mutated (Fig. 3a). This prevents cleavage by the OTU and thus resembles the inhibitory binding of cellular Ub to L-C40A. Furthermore, UbV-CC4 contains an extended C-terminal tail that forms additional contacts with the OTU, resulting in enhanced affinity. Using UbV-CC4, we set out to investigate the potential antiviral effect of blocking CCHFV OTU activity. As a control, a wild-type-like Ub variant was used in which only the C-terminal di-Gly motif was mutated to alanine (UbV-AA). Mutation of this motif in both Ub variants prevents their conjugation to cellular or viral proteins and therefore results in a lower likelihood of interference with normal Ub conjugation.

To confirm that UbV-CC4 interacts with both OTU-wt and OTU-C40A, we used time-resolved fluorescence resonance energy transfer (TR-FRET). HEK293T cells were transfected with plasmids expressing V5-OTU and hemagglutinin-tagged ubiquitin (HA-Ub) or with plasmids expressing V5-OTU and FLAG-UbV-CC4 and were subsequently labeled with a donor or acceptor fluorophore. A plasmid expressing green fluorescent protein (GFP) was used as a control. Close proximity of proteins, such as protein-protein interactions, results in increased intensity of the fluorescent signal. Coexpression of UbV-CC4 with either OTU-wt or OTU-C40A resulted in an increased TR-FRET signal, whereas coexpression of either OTU with GFP did not (Fig. 3b). In contrast, only coexpression of HA-Ub with OTU-C40A resulted in an increased TR-FRET signal, whereas coexpression with OTU-wt did not. This supports the concept that cellular Ub (HA-Ub) binds only to OTU-C40A whereas the synthetic UbV-CC4 also interacts with OTU-wt. We reaffirmed the interaction of UbV-CC4 with OTU-wt using coimmunoprecipitation. Cells were transfected with plasmids encoding HA-OTU-wt and FLAG-UbV-CC4 or the FLAG-UbV-AA control. Pulldown of HA-OTU-wt resulted in detection of FLAG-UbV-CC4 but not FLAG-UbV-AA (Fig. 3c).

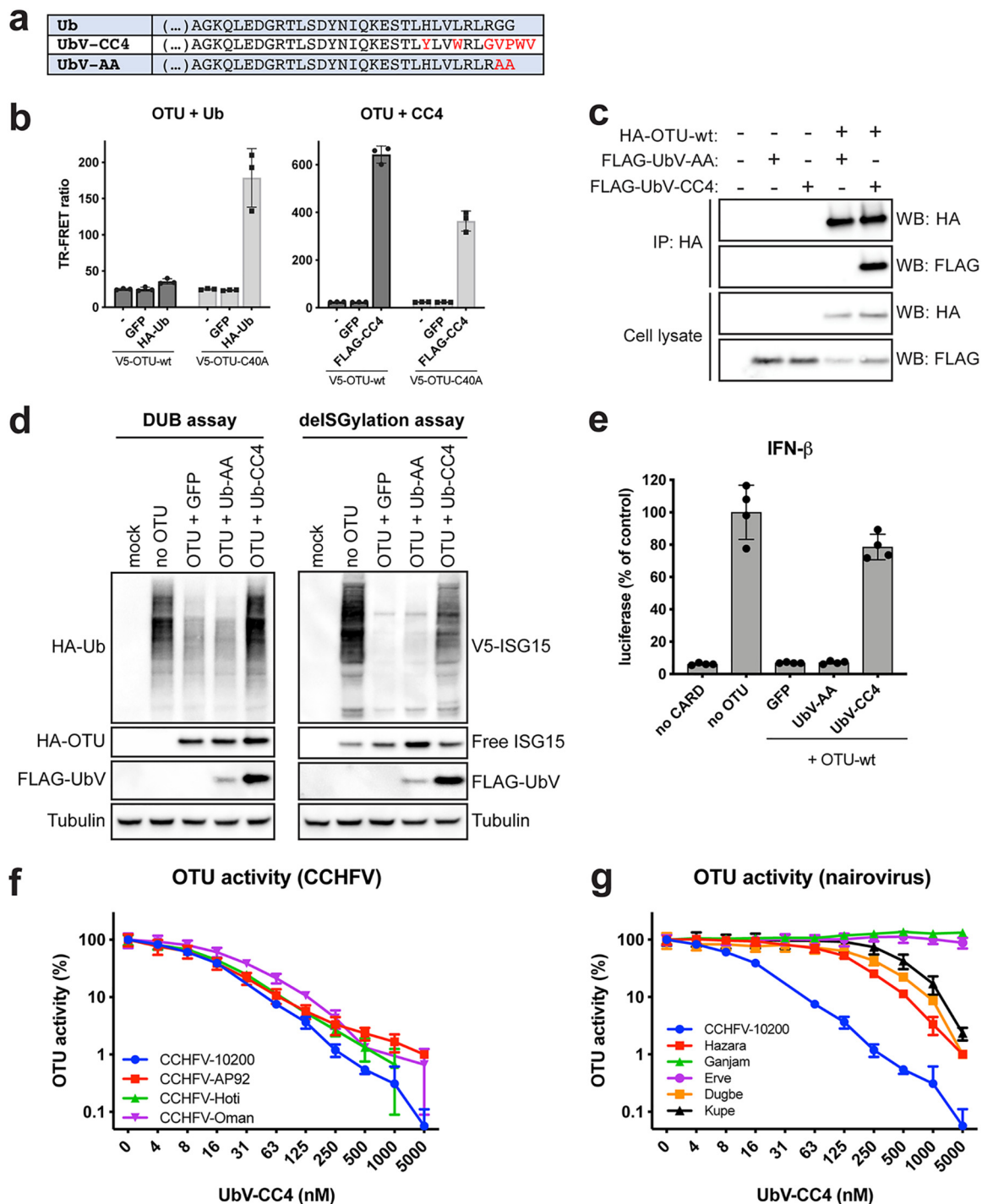


FIG 3 UbV-CC4 blocks CCHFV OTU activity. (a) Alignment of the C-terminal sequences of Ub and the CC4 and AA Ub variants. Residue variations are highlighted in red. (b) Analysis of OTU (wt and C40A) interactions with HA-Ub or UbV-CC4 using TR-FRET. HEK293T cells were cotransfected with plasmids expressing V5-OTU and HA-Ub or plasmids expressing V5-OTU and FLAG-UbV-CC4. A plasmid expressing GFP was used as a control. After 2 days, samples were harvested and incubated with donor and acceptor fluorophores. Protein-protein proximity was determined by measuring the intensity of the fluorescent signal. Data are presented as means \pm SD of results from three replicates. (c) To confirm the interaction of OTU-wt with UbV-CC4, HEK293T cells were transfected with plasmids expressing HA-OTU-wt and FLAG-UbV (FLAG-UbV-AA or FLAG-UbV-CC4). Lysates were immunoprecipitated (IP) with HA antibodies and analyzed by Western blotting (WB). (d) To assess whether UbV-CC4 affects CCHFV OTU activity, Huh7 cells were cotransfected with plasmids encoding HA-Ub (DUB assay) or the proteins required for ISGylation (V5-ISG15, Ube1L, UbcH8, and HERC5). After 48 h, levels of protein ubiquitination and ISGylation were assessed by Western blotting. (e) To assess the effect of UbV-CC4 on OTU-mediated immune suppression in an overexpression assay, Huh7 cells were cotransfected with a reporter plasmid encoding firefly luciferase under the control of the IFN- β promoter, and a plasmid encoding constitutively active RIG-I CARD. After 48 h, luciferase activity was determined as a measure of RIG-I-mediated IFN- β expression. A plasmid expressing *Renilla* luciferase was used for normalization. Data are presented as means \pm SD

(Continued on next page)

We then examined the effects of UbV-CC4 on CCHFV OTU deubiquitinase and deISGylase activity. To visualize cellular ubiquitinated and ISGylated proteins, cells were transfected with plasmids expressing HA-Ub (DUB assay) or V5-ISG15 in combination with the enzymes required for conjugation (Ube1L, UbcH8, and HERC5; deISGylation assay). Analysis of the cellular levels of ISG15 or Ub demonstrates that UbV-CC4 efficiently blocked the OTU-mediated removal of Ub and ISG15 from their protein targets, whereas UbV-AA had no effect on OTU activity (Fig. 3d). Additionally, blocking OTU DUB activity with UbV-CC4 enhanced ubiquitination of the L protein (see Fig. S1 in the supplemental material).

Since CCHFV OTU deubiquitinase activity is sufficient to block RIG-I-mediated type I IFN signaling (8, 9), we investigated if UbV-CC4 could affect OTU-mediated immune suppression in a reporter assay (Fig. 3e). RIG-I-mediated induction of beta IFN (IFN- β) gene expression, measured in cells transfected with plasmids encoding the constitutively active RIG-I CARD domain, and luciferase under the control of the IFN- β promoter, was efficiently blocked by CCHFV OTU. As further support for the idea of UbV-CC4 blocking OTU activity, OTU immune-suppressive activity was prevented by coexpression of UbV-CC4. Taken together, these experiments demonstrated the ability of UbV-CC4 to block proteolytic activity of CCHFV OTU and restore cellular RIG-I signaling.

UbV-CC4 selectively inhibits CCHFV OTUs. The wide geographic distribution of CCHFV is reflected in its considerable genetic diversity. To assess if UbV-CC4 is able to inhibit OTU activity from divergent CCHFV strains and other nairovirus species, we performed *in vitro* OTU activity assays. Increasing concentrations of UbV-CC4 were incubated with purified OTUs and a fluorogenic Ub substrate (ubiquitin 7-amido-4-methylcoumarin [Ub-AMC]). UbV-CC4 inhibited the *in vitro* OTU activity of all tested CCHFV strains (IbAr10200, AP92, Hoti, and Oman) with similar levels of efficiency, with IC_{50} values ranging from 12 to 23 nM (Fig. 3f; see also Table S1 in the supplemental material). In contrast, OTUs from other nairovirus species showed relatively poor or no inhibition by UbV-CC4, demonstrating that UbV-CC4 is specific for all CCHFV strains tested but not for more distantly related viruses (Fig. 3g; see also Table S1).

UbV-CC4 inhibits CCHFV replication. To assess if UbV-CC4-mediated inhibition of OTU activity affects CCHFV replication, we generated A549 cell lines stably expressing UbV-CC4 or control UbV-AA. We analyzed the growth kinetics of a CCHFV-ZsG reporter virus in these cells and measured viral titers and ZsG fluorescence as indicators of viral replication and protein synthesis (Fig. 4a to c) (26). Strikingly, UbV-CC4 robustly reduced ZsG levels at all tested time points, whereas the UbV-AA control did not affect ZsG fluorescence (Fig. 4c). In addition, CCHFV-infected A549-CC4 cells produced very low to undetectable levels of viral progeny, whereas A549-AA cells produced titers similar to those measured for the control cells (unmodified A549 cells; Fig. 4a and b). Infectious titers of CCHFV lacking the ZsG reporter (CCHFV-wt) closely matched the curves determined on the basis of ZsG fluorescence, further supporting quantification of CCHFV-derived ZsG fluorescence to accurately estimate viral growth (Fig. 4a to c). Finally, to ensure that the UbV-CC4-mediated inhibition of CCHFV growth was specific and was not caused by broad antiviral effects of UbV-CC4, we used a Lassa reporter virus (LASV) expressing ZsG (LASV-ZsG) as a control (Fig. 4d). LASV-ZsG growth kinetics are unaffected by UbV-CC4, confirming that UbV-CC4 specifically and potently inhibits CCHFV.

UbV-CC4 inhibits CCHFV replication independently of innate immune responses. Since CCHFV does not require OTU activity for autoproteolytic processing of

FIG 3 Legend (Continued)

of results from four replicates. (f and g) *In vitro* analysis of the effect of UbV-CC4 on OTUs from different CCHFV strains (f) or other nairovirus species (g). Reactions to determine the inhibitory activity of Ub-CC4 against the different OTUs were performed using inhibitor concentrations ranging from 3.9 nM to 5 μ M. OTUs were incubated with the inhibitor for 2 min, and then the reactions were initiated by adding Ub-AMC and were monitored by quantification of the increase in fluorescence. Reaction rates were determined using the linear portion of the curves, and percent inhibition was calculated. IC_{50} and related errors were determined in the SigmaPlot 12 enzyme kinetics module utilizing Michaelis-Menten kinetics (Systat Software, Inc.). Data are presented as means \pm SD of results from three replicates.

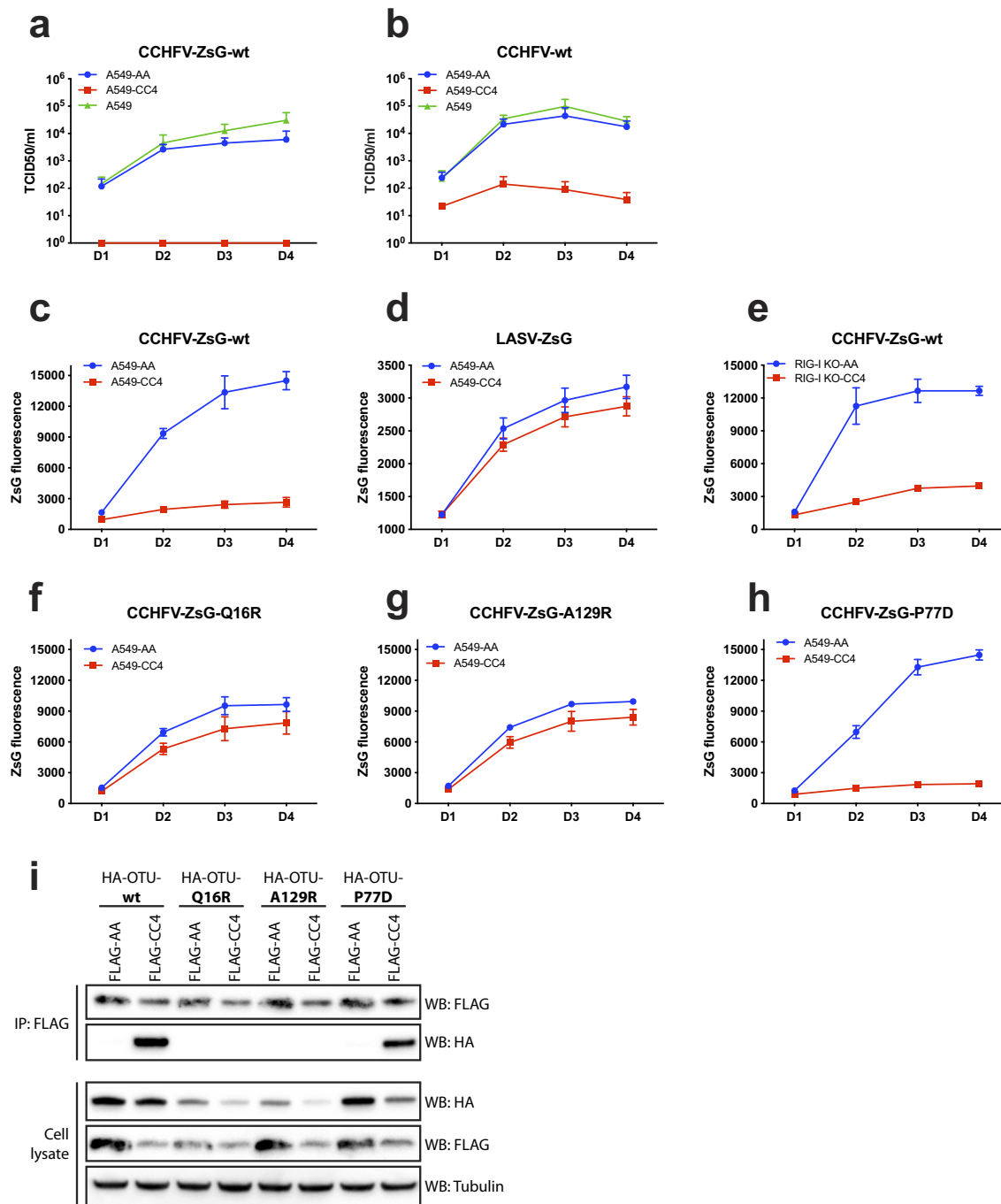


FIG 4 UbV-CC4 can block CCHFV replication in the absence of RIG-I-mediated immune responses. (a and b) To determine the effect of UbV-CC4 on the release of progeny virus, A549 cells stably expressing UbV-AA (A549-AA) or UbV-CC4 (A549-CC4) were infected with either the ZsG reporter virus (CCHFV-ZsG-wt) (a) or the unlabeled parental CCHFV (CCHFV-wt) (b) at an MOI of 0.01. Infectious titers were determined at the indicated time points. Data are presented as means \pm SD of results from three independent experiments performed in triplicate. (c) To assess the effect of UbV-CC4 on viral replication, A549 cells stably expressing UbV-AA or UbV-CC4 were infected with a CCHFV reporter virus (CCHFV-ZsG; MOI of 0.1). (d) LASV-ZsG (MOI of 0.1) was used as a control. ZsG reporter activity was quantified at the indicated time points as a measure of viral replication. Data are presented as means \pm SD of results from three replicates. (e) To determine whether RIG-I signaling is involved in the CC4-mediated suppression of CCHFV replication, A549 RIG-I KO cells stably expressing UbV-AA or UbV-CC4 were infected with CCHFV-ZsG (MOI of 0.1) and ZsG reporter activity was quantified at the indicated time points. Data are presented as means \pm SD of results from three replicates. (f to h) To confirm that direct binding of the UbV-CC4 to the CCHFV OTU is responsible for the inhibition of CCHFV replication, we employed recombinant viruses containing OTU mutations that disrupt binding to Ub (Q16R) or to ISG15 (P77D) or to both Ub and ISG15 (A129R). A549 cells stably expressing UbV were infected with these CCHFV OTU mutants (MOI of 0.1), and ZsG fluorescence was determined as a measure of viral replication at the indicated time points. Data are presented as means \pm SD of results from three replicates. (i) To confirm the interaction of the OTU (mutants) with UbV-CC4, we performed coimmunoprecipitation assays. HEK293T cells were transfected with the indicated plasmids, and cell lysates were harvested after 2 days.

its viral proteins or for polymerase activity (18), we expected that UbV-CC4 would reduce CCHFV infection by interfering with OTU-mediated immune suppression, which would result in enhanced cellular immune responses. A549 cells display robust IFN responses upon CCHFV infection, and previous studies have demonstrated that RIG-I signaling plays a pivotal role in the antiviral cellular response against CCHFV infection (8, 29). To investigate if UbV-CC4-mediated inhibition of CCHFV infection depends on enhanced cellular immune responses, we assessed UbV-CC4 antiviral activity in an A549 RIG-I knockout cell line (RIG-I KO). Using the A549 RIG-I KO cells as a basis, we generated additional cell lines stably expressing UbV-AA or UbV-CC4. Interestingly, robust inhibition of CCHFV was noted even in the absence of RIG-I-mediated antiviral responses (Fig. 4e). This confirms that UbV-CC4 can inhibit CCHFV infection independently of RIG-I.

OTU residues required for Ub binding are critical for UbV-CC4 antiviral activity.

Our data support a model in which binding of cellular Ub to the inactive OTU (C40A) blocks the recovery of infectious CCHFV and binding of UbV-CC4 to OTU-wt mimics this inhibition (Fig. 1, 3, and 4a to c). Specific OTU mutations have been described that selectively disrupt OTU interaction with Ub (Q16R) or with ISG15 (P77D) or both (A129R) (8, 25, 30, 31). Since UbV-CC4 interacts with the OTU in a manner similar to that seen with cellular Ub, we expected that the Q16R and A129R mutations would prevent UbV-CC4 binding to the OTU and therefore would relieve UbV-CC4 inhibition of CCHFV infection. Recombinant viruses containing these OTU mutations were generated and used to infect cells expressing UbV-CC4. As predicted, mutant viruses CCHFV-Q16R and CCHFV-A129R, which are deficient in Ub binding, were not inhibited by UbV-CC4, whereas CCHFV-P77D, which retains significant Ub binding, was inhibited similarly to the wt virus (Fig. 4c and f to h). We confirmed the specific binding of UbV-CC4 to the mutant OTUs by performing coimmunoprecipitation experiments (Fig. 4i). Thus, binding of UbV-CC4 to the OTU domain is required for inhibition of CCHFV infection.

UbV-CC4 disrupts viral RNA transcription and/or replication. To pinpoint the step(s) in the CCHFV replication cycle that is affected by UbV-CC4, we used a minigenome assay and a virus-like particle (VLP) assay. These systems have the advantage of separating various steps of the viral replication cycle potentially affected by UbV-CC4 and can provide insight into its mechanism of action. The VLP assay allows us to address early steps in the replication cycle, such as entry, uncoating, and primary transcription of the encapsidated minigenome. Interestingly, when VLPs were added to UbV-CC4-expressing cells, only a mild reduction in VLP reporter activity compared to the UbV-AA control was detected (Fig. 5a). In order to confirm the VLP results with genuine virus, we used a CCHFV reporter expressing NanoLuciferase (CCHFV-Nluc; Fig. 5b). Overall, UbV-CC4 did not inhibit luciferase expression early in infection, suggesting that UbV-CC4 likely affects viral genome amplification without interfering with entry or primary transcription.

Next, we used a minigenome assay to examine whether UbV-CC4 affects L-RdRp activity (Fig. 5c). UbV-CC4 severely hampered CCHFV minigenome reporter activity, suggesting that UbV-CC4 affects transcription or replication of viral RNA. To confirm that UbV-CC4 interferes with the production of nascent viral RNA, and not simply with the translation thereof, we assessed minigenome RNA levels in the presence of UbV-CC4 (Fig. 5d). Indeed, less viral RNA was produced in the presence of UbV-CC4, whereas UbV-AA did not affect minigenome RNA levels. These experiments demonstrated that UbV-CC4 affects viral transcription and/or replication.

The exact mechanism required for the generation of nascent CCHFV RNA has not been elucidated. However, CCHFV likely replicates its genomic material in a way similar to that of related bunyaviruses. This process entails NP binding to genomic RNA to form ribonucleoprotein (RNP) complexes, which in turn interact with the L protein, resulting in transcription or replication. Regions required for the L-NP interaction have been identified on both the N and C termini of the CCHFV L protein (32). We investigated the possibility that UbV-CC4 interferes with CCHFV transcription and/or replication by disrupting the formation of RNP complexes by assessing the interaction between L and

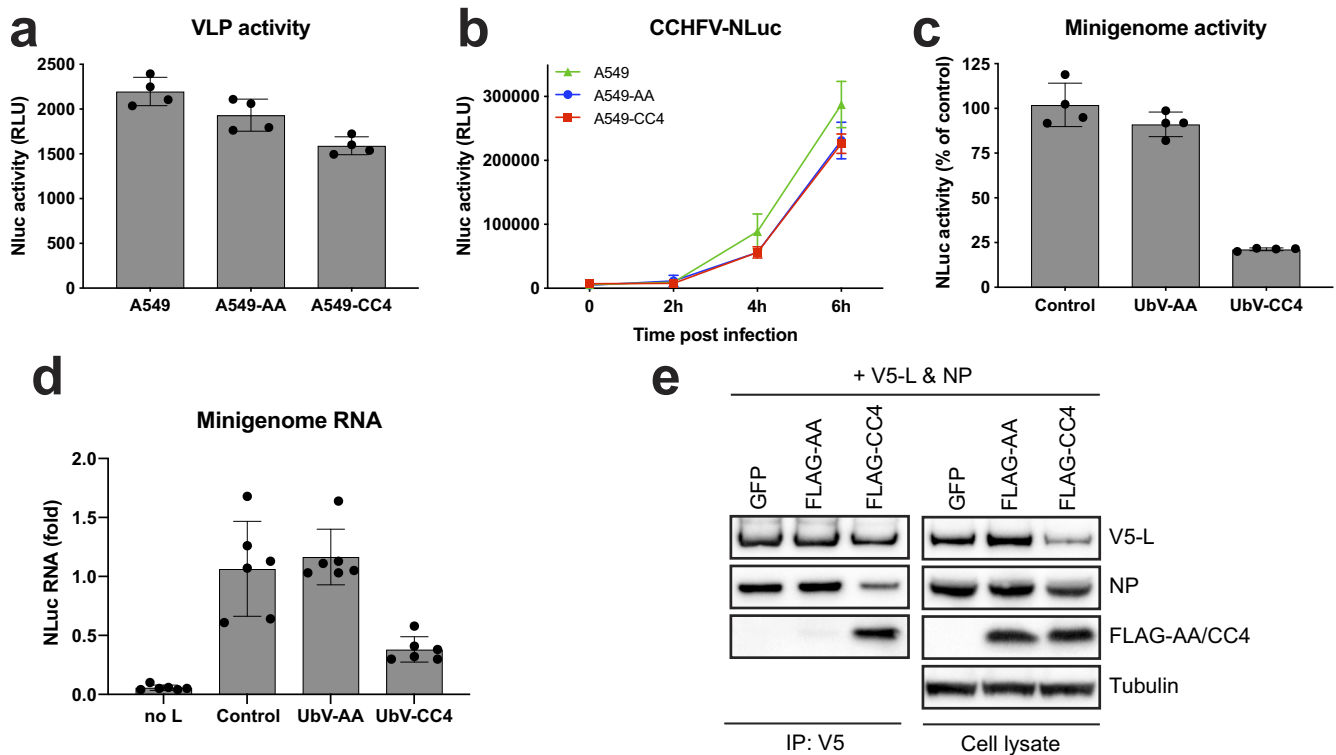


FIG 5 UbV-CC4 inhibits viral RNA transcription and/or replication. (a) VLPs were used to determine whether UbV-CC4 affects CCHFV entry. VLPs were generated by transfecting Huh7 cells with plasmids encoding CCHFV NP, GPC, codon-optimized L, T7 polymerase, and a NanoLuc (Nluc)-encoding minigenome. VLP-containing supernatants were harvested after 3 days and transferred to A549 cells stably expressing UbV-AA or UbV-CC4. NanoLuc activity was quantified the next day as a measure of VLP activity. Data are presented as means \pm SD of results from four replicates. RLU, relative light units. (b) To analyze if UbV-CC4 affects early replication steps after entry, we used a NanoLuc-expressing reporter virus (CCHFV-NLuc). A549 cells stably expressing UbV were infected (MOI of 5), and NanoLuc activity was determined at the indicated time points. Data are presented as means \pm SD of results from three replicates. (c) A minigenome assay was used to determine if UbV-CC4 directly affects CCHFV genome amplification. Huh7 cells were cotransfected with plasmids encoding CCHFV NP, codon-optimized L, T7 polymerase, and a NanoLuc-encoding minigenome. After 2 days, NanoLuc activity was quantified as a measure of CCHFV RdRp activity. Constitutively active *Renilla* luciferase was used as a transfection control. Data are presented as means \pm SD of results from three replicates. (d) To analyze CCHFV minigenome RNA levels, RNA was isolated from Huh7 cells transfected with the minigenome components described for panel c. Minigenome RNA levels were quantified using qRT-PCR. Data are presented as means \pm SD of results from six replicates. (e) To investigate if UbV-CC4 binding to the OTU interferes with L-NP interaction, HEK293T cells were transfected with plasmids expressing CCHFV NP, codon-optimized V5-L, and UbV-AA or UbV-CC4. L-NP interaction was assessed by coimmunoprecipitating V5-L and determining the associated NP levels.

NP in the presence of UbV-CC4. Cells were transfected with plasmids expressing CCHFV V5-L, NP, and FLAG-UbV-AA or FLAG-UbV-CC4. Lysates were immunoprecipitated using V5 and were analyzed by Western blotting. This assay demonstrated that less NP is associated with V5-L in the presence of UbV-CC4 (Fig. 5e), supporting a model where UbV-CC4 interferes with the formation of CCHFV replication complexes.

DISCUSSION

Various highly pathogenic RNA viruses, including CCHFV, Middle East respiratory syndrome coronavirus (MERS-CoV), and severe acute respiratory syndrome coronavirus (SARS-CoV), encode DUB domains that contain deubiquitinase and deISGylase activity (7, 8, 14, 33). These viral DUBs likely contribute to viral pathogenesis by suppressing innate immune responses. In addition, DUBs of positive-strand RNA viruses are essential for the viral polyprotein processing required for polymerase maturation. Despite being part of the RNA polymerase, DUBs encoded by negative-strand RNA viruses of the family *Nairoviridae* (termed OTUs) are dispensable for polymerase activity (18). Instead, suppression of host immune responses appears to be the main function of nairovirus OTUs. Here, by mutating the OTU and employing a synthetic Ub variant (UbV-CC4), we characterized the effects of disrupting OTU activity on CCHFV infection. Unexpectedly, we discovered that solely mutating the OTU catalytic site (C40A) abolishes viral propagation, as the prolonged binding to its substrate Ub interferes with transcription

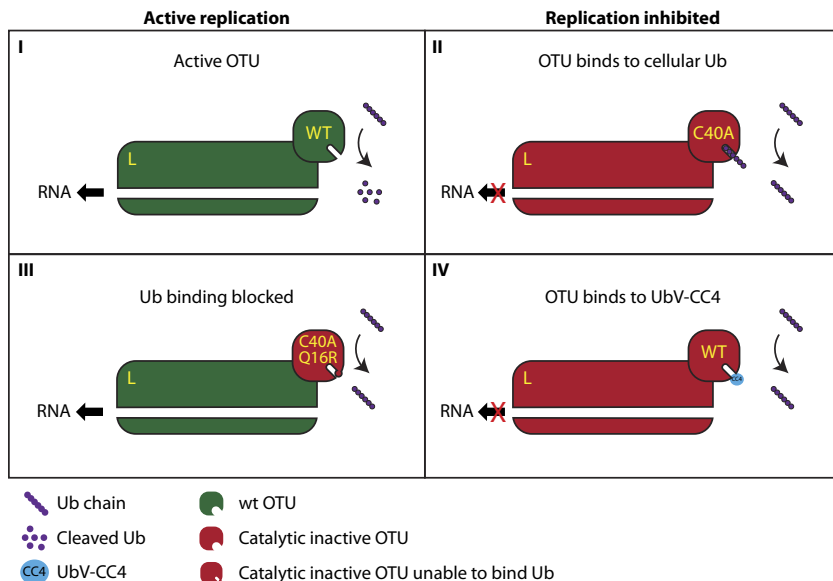


FIG 6 Schematic model of OTU stable interaction with cellular Ub or UbV-CC4 leading to the block of viral RNA replication. (Panel I) Wild-type OTU possesses deubiquitinase activity, which allows the deconjugation of Ub chains. (Panel II) Catalytically inactive OTU (C40A) can engage ubiquitinated substrates but is not able to cleave Ub chains. The formation of a Ub-OTU complex interferes with viral replication. (Panel III) Adding an additional mutation that prevents binding to Ub (Q16R) to catalytically inactive OTU (C40A) disrupts the formation of Ub-OTU complexes and restores viral replication. (Panel IV) Binding of a synthetic Ub variant (UbV-CC4) to wild-type OTU interferes with viral replication.

and/or genome amplification. Similarly, a noncleavable synthetic Ub variant (UbV-CC4) inhibits propagation of wild-type CCHFV (Fig. 6).

CCHFV propagation in the absence of OTU catalytic activity (C40A) was restored by inclusion of an additional mutation that prevents Ub binding (Q16R), suggesting that binding of the inactive OTU to cellular Ub inhibits viral growth. Importantly, this does not appear to be mediated by a simple difference in affinity levels between OTU-wt and OTU-C40A, as isothermal titration calorimetry results showed no change in the favorability of binding mono-Ub between OTU-wt and OTU-C40A (see Table S2 in the supplemental material). However, cellular Ub is often found as polymeric chains, and CCHFV OTU has been demonstrated to cleave these Ub chains (34). Although structural studies have only revealed interactions between the CCHFV OTU and a single Ub within a well-characterized binding site, there is biochemical evidence suggesting the presence of a secondary binding site in nairovirus OTUs that facilitates interactions with Ub chains (35). When OTU-wt cleaves the Ub chains, it converts a single high-affinity interaction into two lower-affinity ones that facilitate substrate release. On the other hand, OTU-C40A is unable to cleave Ub chains, resulting in a prolonged association with Ub and subsequent blocking of virus replication. Similarly, UbV-CC4 blocks viral transcription and/or replication by prolonged association with OTU-wt due to the absence of the consensus cleavage motif combined with the presence of extra interacting residues increasing binding affinity. In conclusion, prolonged Ub-OTU association, due to the absence of either OTU catalytic activity (C40A) or the Ub consensus cleavage motif in UbV-CC4, appears sufficient to inhibit CCHFV transcription and/or replication.

We previously demonstrated that an intact OTU domain is not required for CCHFV RdRp activity (8, 18), and the generation of recombinant CCHFV containing a catalytically inactive OTU further confirms that OTU protease activity should be considered accessory to virus replication. In fact, CCHFV-C40A/Q16R was easily propagated in IFN-deficient cells and was pathogenic to IFNAR^{-/-} mice. However, weight loss and mortality were slightly delayed compared to mice infected with CCHFV-wt, and two animals survived CCHFV-C40A/Q16R infection (Fig. 2). Antiviral responses independent

of type I IFN, including the upregulating of certain ISGs, have been described in immunocompromised animals and may be responsible for this observed *in vivo* attenuation (36, 37).

Unexpectedly, we found that occupying the OTU with UbV-CC4 resulted in strong inhibition of CCHFV transcription and/or replication. This was a notable finding, as CCHFV does not require autoproteolytic processing of its viral RNA polymerase, and inhibition of its DUB was therefore expected to interfere only with its ability to suppress host immunity. Mechanistically, inhibition of CCHFV by UbV-CC4 was characterized by a strong reduction of CCHFV minigenome reporter activity (Fig. 5c and d), whereas early infection events were minimally affected (Fig. 5a and b). Our data support a model in which prolonged binding of the OTU to Ub(V) interferes with the formation of new RNP complexes, thus affecting viral transcription and/or genome amplification. Formation of CCHFV RNP complexes involves interactions of viral RNA, NP, and the L protein. In the presence of UbV-CC4, less NP was associated with L protein in transfected cells, suggesting a possible defect in RNP complex formation (Fig. 5e). NP binding occurs at two distinct sites located at the N and C termini of L (32), which might be differently affected by binding of the OTU to Ub/UbV-CC4, possibly explaining the residual interaction between NP and L detected in the presence of UbV-CC4. The CCHFV L protein harboring the RNA polymerase and OTU is an unusually large protein (~450 kDa), and the tridimensional arrangement of the OTU domain relative to the RNA polymerase is unknown. Therefore, the consequences of prolonged OTU binding to Ub/UbV-CC4 with respect to polymerase conformation and activity are presently unpredictable. It is conceivable that Ub/UbV-CC4 binding to the OTU domain might simply lock the polymerase in an inactive state, preventing RNA synthesis. Structural data combined with *in vitro* assays will be necessary to further elucidate the precise mechanism of OTU-UbV-CC4 complex interference in transcription and replication.

We found that OTU binding to Ub was responsible for the block in virus growth in the absence of protease activity. Similarly, specific inhibition of CCHFV-OTU with UbV-CC4 directly interfered with viral propagation, further demonstrating that prolonged association of the OTU with cellular Ub or the UbV-CC4 inhibitor is sufficient to severely impair CCHFV growth. UbV-CC4 inhibits *in vitro* OTU activity of genetically diverse CCHFV strains but has little to no effect on the OTU activity of other nairovirus species (Fig. 3f and g). The nairoviral OTU domain displays a high degree of sequence diversity, potentially affecting the binding affinity of UbV-CC4. For example, UbV-CC4's Tyr⁶⁸ improves hydrophobic packing with OTU residues Thr¹⁰, Val¹², and Val¹⁸ (28). Thr¹⁰ is conserved across the four tested CCHFV OTUs, whereas the other tested nairovirus species predominantly encode a glutamic acid at that position. In addition, OTU amino acids 149 and 150 appear to interact extensively with the UbV-CC4 tail, and this region displays a high level of sequence variation between nairovirus species. Indeed, the four tested CCHFV strains all contain a Gln¹⁴⁹, whereas the other nairovirus species do not.

Drug development for CCHFV is a public health priority, as no specific therapeutics with demonstrated efficacy are currently available. We demonstrate that stable occupancy of the OTU by UbV-CC4 not only enhanced host antiviral responses but also decreased viral growth by interfering with the formation of RNP complexes. This illustrates that targeting the viral OTU of negative-strand RNA viruses is a viable antiviral strategy. Therefore, our data provide an important framework for researching and developing small-molecule inhibitors targeting the OTU. To recapitulate the OTU-UbV-CC4 interactions, a candidate drug would need to inhibit OTU catalytic activity while maintaining or enhancing the high level of affinity of the OTU for Ub chains.

Taking the results together, our study demonstrated that stable occupancy of the OTU blocks viral transcription/replication and that inhibiting the OTU suppresses its IFN antagonist function, thereby disrupting these 2 critical viral processes for CCHFV pathogenesis. This report demonstrates the antiviral potential of targeting a viral OTU and serves as an important proof of concept for the rational design of OTU-specific antivirals that block virus infection at multiple levels.

MATERIALS AND METHODS

Biosafety and ethics statement. All animal procedures were approved by the CDC Institutional Animal Care and Use Committee and conducted in accordance with the Guide for the Care and Use of Laboratory Animals at an AAALAC-accredited facility (38). Procedures conducted with LASV-, CCHFV-, or CCHFV-infected animals were performed in biosafety level 4 facilities at the Centers for Disease Control and Prevention (Atlanta, GA, USA). Experiments involving cDNA encoding viral sequences were performed in accordance with approved Institutional Biosafety Committee protocols.

Cells. Huh7, A549, A549 RIG-I KO, BSR-T7/5, and HEK293T cells were maintained in Dulbecco's modified Eagle medium (DMEM) supplemented with 5% to 10% fetal calf serum, 1 mM sodium pyruvate, 1% nonessential amino acids, and 100 U/ml antibiotics. BSR-T7/5 cells were a gift from K. K. Conzelmann (Ludwig-Maximilian-Universität, Munich, Germany). A549-dual RIG-I knockout cells were obtained from InvivoGen.

Viruses. Recombinant IbAr10200 CCHFV was generated as previously described (GenBank accession no. [KJ648914](#), [KJ648915](#), and [KJ648913](#)) (8, 39). Briefly, Huh7 cells were transfected with plasmids encoding the full-length L, M, and S genome segments under the control of a T7 promoter and with helper plasmids expressing CCHFV NP, codon-optimized L protein, and T7 polymerase. Viruses with mutated OTUs were generated by adding point mutations to the pT7-L plasmids using site-directed mutagenesis before virus rescue. ZsGreen1-expressing reporter CCHFV, which was described previously (26), contains the ZsGreen1 coding sequence fused to NP, separated by a P2A sequence. NanoLuc-expressing CCHFV was generated using the same cloning strategy. The recombinant LASV reporter (LASV-ZsG) was described previously (40). All recombinant viruses were verified with deep-sequencing technology using a MiniSeq system (Illumina).

Virus infectivity was measured by titration in BSR-T7/5 cells either by the use of ZsG as a readout or by the use of immunofluorescence with anti-CCHFV polyclonal antibodies (hyperimmune mouse ascetic fluid [generated in-house]), and the median 50% tissue culture infective dose (TCID₅₀) was determined.

Animal experiments. Female B6.129S2-*Irfnar1*^{tm1Agt}/Mmjax mice (MMRRC 032045-JAX) were housed in a climate-controlled laboratory with a 12-h day/12-h night cycle. All animals were given sterile water and food *ad libitum* and were group housed (4/cage) on autoclaved corn cob bedding (Bed-o-Cobs; Anderson Lab Bedding) (1/4 in. thick) in an isolator-caging system (Thoren Caging, Inc., Hazleton, PA, USA) with a HEPA-filtered inlet and exhaust air supply. The cage environment was enriched with shredded paper and cotton nestlets. To assess the various CCHFV mutant viruses, animals (6.5 weeks of age, 8 mice per group) were inoculated subcutaneously in the interscapular region with 10² TCID₅₀ of CCHFV diluted in DMEM. Mice were humanely euthanized at the indicated time points or when clinical illness scores based on piloerection, decreased activity, neurological signs (e.g., ataxia, paresis/paralysis), dehydration, dyspnea, and/or weight loss (>20% from baseline at -1 dpi) indicated that the animal was in distress or in the terminal stages of disease. Differences in weight change from baseline according to day postinfection and survival were statistically analyzed by multiple *t* tests, with significance determined using the Holm-Sidak method ($\alpha = 0.05$) and the log rank (Mantel-Cox) test, respectively (GraphPad Prism 8).

Quantitative RT-PCR. Nucleic acids were extracted from blood and homogenized tissues using MagMax technologies (Thermo Fisher Scientific) and a 96-well ABI MagMAX extraction platform. RNA was quantified using one-step real-time PCR (RT-PCR) targeting the IbAr10200 nucleoprotein gene sequence (primer and probe sequences available on request), and data were normalized to 18S RNA levels. Viral S segment copy numbers were determined using standards prepared from S segment RNA transcribed *in vitro*.

TR-FRET. UbV-CC4 and the unmodified UbV-AA control have been described previously (28). The genes were synthesized and inserted into a pcDNA3 vector. Both variants contain an N-terminal 6×His tag and a FLAG tag. The OTU domain (amino acids 1 to 168) was synthesized and cloned into pcDNA3.1 containing a C-terminal HA tag (all from GenScript).

Protein-protein interactions were examined using time-resolved fluorescence energy transfer (TR-FRET). HEK293T cells were seeded in 10-cm² dishes (5 × 10⁶) and transfected with pcDNA-V5-OTU (wt or C40A) and with pcDNA-FLAG-UbV-CC4, pcDNA-HA-Ub, or pcDNA-eGFP. Two days posttransfection, cells were harvested in Triton lysis buffer (1% Triton X-100, 20 mM Tris-HCl, 2.5 mM MgCl₂) and clarified by centrifugation (1 min at 13,000 rpm). Lysates were incubated at room temperature with TR-FRET donor/acceptor pairs. To examine the interaction of V5-OTU with HA-Ub, lysates were incubated with anti-V5-Eu (donor) and anti-HA-d2 (acceptor). To examine the interaction of V5-OTU with FLAG-CC4, lysates were incubated with anti-V5-Eu (donor; Perkin Elmer) and anti-FLAG M2-d2 (acceptor; Cisbio). Fluorescence transfer was determined using a Synergy 4 plate reader (Bio-Tek) and calculated as the ratio of donor excitation to acceptor excitation.

Coimmunoprecipitation. HEK293T cells were seeded in 10-cm² dishes (5 × 10⁶) and transfected with the indicated plasmids. If necessary, the total amount of plasmid DNA was supplemented with pcDNA-eGFP. All transfections were performed using TransIT-LT1 (Mirus) following the manufacturer's instructions. After 2 to 3 days, cells were harvested and lysed in Triton lysis buffer (1% Triton X-100, 20 mM Tris-HCl, 2.5 mM MgCl₂). Clarified supernatants were incubated with anti-HA, anti-FLAG, or anti-V5 magnetic beads (1.5 h at 4°C) and washed with high-salt Triton lysis buffer (1% Triton X-100, 20 mM Tris-HCl, 2.5 mM MgCl₂, 500 mM NaCl). Proteins were eluted from the beads by adding 2× Laemmli sample buffer and heating the sample at 50°C for 10 min. Proteins were subsequently separated on 4% to 12% Bis-Tris SDS-PAGE gels and transferred to nitrocellulose membranes using a transblot system (Bio-Rad).

Western blotting and antibodies. Cell lysates were harvested in 2× Laemmli sample buffer and heated for 10 min at 95°C. Proteins were subsequently separated on 4% to 12% Bis-Tris or Tris-acetate SDS-PAGE gels and were then transferred to nitrocellulose membranes using a transblot system (Bio-Rad). The following antibodies were used in this study: CCHFV anti-NP (04-0011; IBT BioServices) and anti-V5 (R960CUS), anti-HA (71-5500), and anti-FLAG (32-6700) (all Thermo Fisher). Tubulin (T5169; Sigma) was used as a loading control marker. Primary antibodies were detected with SuperSignal West Dura Fast Western blot kits (Thermo Fisher). Protein bands were visualized using a ChemiDoc MP system (Bio-Rad).

OTU activity in transfected cells. OTU activity was determined by cotransfecting Huh7 cells with pcDNA-HA-Ub (DUB assay) or with the following plasmids encoding proteins required for ISGylation: pcDNA-Ube1L, pcDNA-UbCH8, pcDNA-NTAP-HERC5 (J. Huijbregtse, University of Texas at Austin), and pcDNA-V5-hISG15 (GenScript). To assess the effect of the UbV on OTU activity, pcDNA-eGFP, pcDNA-FLAG-AA, or pcDNA-FLAG-CC4 was cotransfected with a plasmid expressing CCHFV-OTU. All plasmid transfections were performed using Trans-IT LT1 transfection reagent (Mirus). Ub and ISG15 conjugation levels were determined 48 h posttransfection by Western blotting.

RIG-I luciferase reporter assay. The RIG-I-mediated IFN- β response was assessed by cotransfecting Huh7 cells with a plasmid encoding RIG-I CARD (S. Best, Rocky Mountain Laboratories) and a reporter plasmid encoding firefly luciferase under the control of the IFN- β promoter (p125-luc; T. Fujita, Kyoto University). A plasmid constitutively expressing *Renilla* luciferase was used for transfection normalization. Plasmids encoding the CCHFV OTU and the ubiquitin variants were cotransfected to assess their effect on the RIG-I-mediated IFN- β response. Firefly activity and *Renilla* luciferase activity were quantified using a Dual-Glo luciferase assay system (Promega) in combination with a Synergy 4 plate reader (Bio-Tek).

Inhibition of *in vitro* OTU activity. Nairovirus OTUs were expressed and purified as previously described (30). UbV-CC4 in vector pET-15b was transformed into BL21(DE3) *Escherichia coli* cells and grown to an optical density (OD) of 0.6 to 0.8. Expression was induced with 0.5 mM IPTG (isopropyl- β -D-thiogalactopyranoside) at 18°C overnight. Cells were pelleted by centrifugation at 5,000 × *g* for 10 min and stored at –80°C. The pellet was resuspended in buffer A (75 mM NaCl, 50 mM sodium acetate, 25 mM HEPES [pH 6.8]) supplemented with 5 mg of lysozyme at 4°C for 30 min. The cells were lysed by sonication at 50% power with a 50% duty cycle for 6 min. The lysate was centrifuged at 48,000 × *g*, and the supernatants were pooled and filtered through a 0.8- μ m-pore-size filter. The clarified lysate was poured over a nickel-nitrilotriacetic acid (Ni-NTA) column (Gold Biotechnology, Olivette, MO) equilibrated with buffer A. The column was washed with 5 column volumes of buffer A supplemented with 10 mM imidazole, followed by protein elution with buffer A supplemented with 300 mM imidazole. The eluate was subsequently filtered through a 0.2- μ m-pore-size filter and further purified by size exclusion using a Superdex 75 column (GE Healthcare) equilibrated in buffer B (100 mM NaCl, 5 mM HEPES [pH 7.2], 2 mM dithiothreitol [DTT]). Samples of fractions containing the absorbance peaks were analyzed by SDS-PAGE. Fractions containing pure UbV-CC4 were pooled and concentrated and then subsequently flash-frozen in 5% glycerol and stored at –80°C.

Reactions to determine the inhibitory effects of UbV-CC4 on different OTUs were performed at 25°C using a CLARIOstar plate reader (BMG Labtech). The reactions were run with a total volume of 30 μ l in a mixture containing 100 mM NaCl, 50 mM HEPES (pH 7.5), 5 mM DTT, and 0.01% bovine serum albumin (BSA) with 4 nM OTU and 1 μ M ubiquitin 7-amido-4-methylcoumarin (Ub-AMC; Boston Biochem, MA). Each OTU was tested in triplicate against UbV-CC4 concentrations ranging from 3.9 nM to 5 μ M. OTUs were incubated with UbV-CC4 for 2 min, and the reactions were initiated by adding Ub-AMC and were monitored by the increase in fluorescence. Reaction rates were determined using the linear portion of the curves, percent inhibition was calculated, and IC₅₀ and related errors were determined using the SigmaPlot 12 enzyme kinetics module utilizing Michaelis-Menten kinetics (Systat Software, Inc.).

UbV-expressing stable cell lines. Cells stably expressing UbV-AA or UbV-CC4 were generated using lentiviruses. First, Gateway technology was used to transfer the UbV genes into pSCRPSY lentiviral vectors containing red fluorescent protein (RFP) and a puromycin resistance gene (C. Rice, The Rockefeller University, NY). Lentivirus was generated by transfecting Lenti-X 293 cells (Clontech) with packaging vectors expressing vesicular stomatitis virus protein G (VSV-G), pPAX2-HIV-gag (Addgene), and pSCRPSY-FLAG-UbV using XtremeGene9 (Roche). After 3 days, supernatants were collected, centrifuged 5 min at 1,000 × *g*, and filtered through a 0.45- μ m-pore-size filter. HEPES and Polybrene were added to reach final concentrations of 20 mM and 4 μ g/ml, respectively. Lentiviruses were stored at –80°C until further use. Stable A549 and A549-RIG-I KO cell lines were generated by puromycin selection after transduction.

Minigenome assay. The CCHFV minigenome assay used here was described previously (41). Briefly, the CCHFV minigenome encodes the NanoLuc gene flanked by CCHFV noncoding regions under the control of a T7 polymerase. To analyze RdRp activity, Huh7 cells were transfected with plasmids encoding the minigenome, CCHFV NP, codon-optimized CCHFV L, T7 polymerase, and a firefly luciferase transfection control (pRL3; Promega) using Transit-LT1 (Mirus). After 48 h, luciferase activity was assessed using a Nano-Glo luciferase assay system (Promega) to detect NanoLuc signal or a luciferase assay system (Promega) to detect firefly luciferase signal. All luminescence readings were carried out using a Synergy 4 plate reader (Bio-Tek).

CCHFV minigenome RNA levels were analyzed by extracting RNA from transfected Huh7 cells using MagMAX RNA isolation reagents (Thermo Fisher Scientific). CCHFV minigenome RNA was quantified using a quantitative real-time PCR (qRT-PCR) assay targeting NanoLuc (Integrated DNA Technologies; primer and probe sequences available on request) and normalized to a housekeeping gene (IPO8; Thermo Fisher Scientific).

Virus-like particle (VLP) assay. Generation of CCHF VLPs has been described previously (41). Briefly, Huh7 cells were transfected with the same plasmid combination as was used in the minigenome assay,

with the addition of a plasmid expressing codon-optimized GPC. VLP-containing supernatant was harvested 3 days posttransfection and transferred to A549 cells stably expressing UbV-CC4 or UbV-AA. NanoLuc activity was determined the next day as a measure of VLP activity.

SUPPLEMENTAL MATERIAL

Supplemental material for this article may be found at <https://doi.org/10.1128/mBio.01065-19>.

FIG S1, TIF file, 0.2 MB.

TABLE S1, DOCX file, 0.01 MB.

TABLE S2, DOCX file, 0.01 MB.

ACKNOWLEDGMENTS

We thank Tatyana Klimova for assistance in editing the manuscript.

This study was supported by the Centers for Disease Control and Prevention (CDC) and a CDC foundation project funded by National Institute of Allergy and Infectious Diseases (NIAID) grant R01AI109008.

The findings and conclusions in this report are ours and do not necessarily represent the official position of the Centers for Disease Control and Prevention.

REFERENCES

- Spengler JR, Bergeron É, Rollin PE. 2016. Seroepidemiological studies of Crimean-Congo hemorrhagic fever virus in domestic and wild animals. *PLoS Negl Trop Dis* 10:1–28. <https://doi.org/10.1371/journal.pntd.0004210>.
- Spengler JR, Bergeron E, Spiropoulou CF. 2019. Crimean-Congo hemorrhagic fever and expansion from endemic regions. *Curr Opin Virol* 34:70–78. <https://doi.org/10.1016/j.coviro.2018.12.002>.
- Estrada-Peña A, Ruiz-Fons F, Acevedo P, Gortazar C, de la Fuente J. 2013. Factors driving the circulation and possible expansion of Crimean-Congo haemorrhagic fever virus in the western Palearctic. *J Appl Microbiol* 114:278–286. <https://doi.org/10.1111/jam.12039>.
- García Rada A. 2016. First outbreak of Crimean-Congo haemorrhagic fever in Western Europe kills one man in Spain. *BMJ* 4891:i4891.
- Negredo A, de la Calle-Prieto F, Palencia-Herrejón E, Mora-Rillo M, Astray-Mochales J, Sánchez-Seco MP, Bermejo Lopez E, Menárguez J, Fernández-Cruz A, Sánchez-Artola B, Keough-Delgado E, Ramírez de Arellano E, Lasala F, Milla J, Fraile JL, Ordobás Gavín M, Martínez de la Gándara A, López Perez L, Díaz-Díaz D, López-García MA, Delgado-Jimenez P, Martín-Quirós A, Trigo E, Figueira JC, Manzanares J, Rodríguez-Baena E, García-Comas L, Rodríguez-Fraga O, García-Arenzana N, Fernández-Díaz MV, Cornejo VM, Emmerich P, Schmidt-Chanasit J, Arribas JR. 2017. Autochthonous Crimean-Congo hemorrhagic fever in Spain. *N Engl J Med* 377:154–161. <https://doi.org/10.1056/NEJMoA1615162>.
- World Health Organization. 2013. Crimean-Congo haemorrhagic fever. <https://www.who.int/news-room/fact-sheets/detail/crimean-congo-haemorrhagic-fever>. Accessed 1 April 2019.
- Frias-Staheli N, Giannakopoulos NV, Kikkert M, Taylor SL, Bridgen A, Paragas J, Richt JA, Rowland RR, Schmaljohn CS, Lenschow DJ, Snijder EJ, García-Sastre A, Virgin HW. 2007. Ovarian tumor domain-containing viral proteases evade ubiquitin- and ISG15-dependent innate immune responses. *Cell Host Microbe* 2:404–416. <https://doi.org/10.1016/j.chom.2007.09.014>.
- Scholte FEM, Zivcec M, Dzimianski JV, Deaton MK, Spengler JR, Welch SR, Nichol ST, Pegan SD, Spiropoulou CF, Bergeron É. 2017. Crimean-Congo hemorrhagic fever virus suppresses innate immune responses via a ubiquitin and ISG15 specific protease. *Cell Rep* 20:2396–2407. <https://doi.org/10.1016/j.celrep.2017.08.040>.
- van Kasteren PB, Beugeling C, Ninaber DK, Frias-Staheli N, van Boheemen S, Garcia-Sastre A, Snijder EJ, Kikkert M. 2012. Arterivirus and nairovirus ovarian tumor domain-containing deubiquitinases target activated RIG-I to control innate immune signaling. *J Virol* 86:773–785. <https://doi.org/10.1128/JVI.01859-09>.
- Kayagaki N, Phung Q, Chan S, Chaudhari R, Quan C, O'Rourke KM, Eby M, Pietras E, Cheng G, Bazan JF, Zhang Z, Arnott D, Dixit VM. 2007. DUBA: a deubiquitinase that regulates type I interferon production. *Science* 318:1628–1632. <https://doi.org/10.1126/science.1145918>.
- Makarova KS, Aravind L, Koonin EV. 2000. A novel superfamily of predicted cysteine proteases from eukaryotes, viruses and Chlamydia pneumoniae. *Trends Biochemistry Sci* 25:50–52. [https://doi.org/10.1016/S0968-0004\(99\)01530-3](https://doi.org/10.1016/S0968-0004(99)01530-3).
- Kinsella E, Martin SG, Grolla A, Czub M, Feldmann H, Flick R. 2004. Sequence determination of the Crimean-Congo hemorrhagic fever virus L segment. *Virology* 321:23–28. <https://doi.org/10.1016/j.virol.2003.09.046>.
- Holzer B, Bakshi S, Bridgen A, Baron MD. 2011. Inhibition of interferon induction and action by the nairovirus Nairobi sheep disease virus/Ganjam virus. *PLoS One* 6:e28594. <https://doi.org/10.1371/journal.pone.0028594>.
- Mielech AM, Kilianski A, Baez-Santos YM, Mesecar AD, Baker SC. 2014. MERS-CoV papain-like protease has deISGylating and deubiquitinating activities. *Virology* 450–451:64–70. <https://doi.org/10.1016/j.virol.2013.11.040>.
- Zheng D, Chen G, Guo B, Cheng G, Tang H. 2008. PLP2, a potent deubiquitinase from murine hepatitis virus, strongly inhibits cellular type I interferon production. *Cell Res* 18:1105–1113. <https://doi.org/10.1038/cr.2008.294>.
- Clementz MA, Chen Z, Banach BS, Wang Y, Sun L, Ratia K, Baez-Santos YM, Wang J, Takayama J, Ghosh AK, Li K, Mesecar AD, Baker SC. 2010. Deubiquitinating and interferon antagonism activities of coronavirus papain-like proteases. *J Virol* 84:4619–4629. <https://doi.org/10.1128/JVI.02406-09>.
- Chenon MM, Camborde L, Cheminant S, Jupin I. 2012. A viral deubiquitylating enzyme targets viral RNA-dependent RNA polymerase and affects viral infectivity. *EMBO J* 31:741–753. <https://doi.org/10.1038/emboj.2011.424>.
- Bergeron E, Albariño CG, Khristova ML, Nichol ST. 2010. Crimean-Congo hemorrhagic fever virus-encoded ovarian tumor protease activity is dispensable for virus RNA polymerase function. *J Virol* 84:216–226. <https://doi.org/10.1128/JVI.01859-09>.
- Durfee LA, Lyon N, Seo K, Huibregtse JM. 2010. The ISG15 conjugation system broadly targets newly synthesized proteins: implications for the antiviral function of ISG15. *Mol Cell* 38:722–732. <https://doi.org/10.1016/j.molcel.2010.05.002>.
- Dastur A, Beaudenon S, Kelley M, Krug RM, Huibregtse JM. 2006. Herc5, an interferon-induced HECT E3 enzyme, is required for conjugation of ISG15 in human cells. *J Biol Chem* 281:4334–4338. <https://doi.org/10.1074/jbc.M512830200>.
- Zou W, Zhang DE. 2006. The interferon-inducible ubiquitin-protein isopeptide ligase (E3) EFP also functions as an ISG15 E3 ligase. *J Biol Chem* 281:3989–3994. <https://doi.org/10.1074/jbc.M510787200>.
- Ganesan M, Poluektova LY, Tuma DJ, Kharbanda KK, Osna NA. 2016. Acetaldehyde disrupts interferon alpha signaling in hepatitis C virus-

- infected liver cells by up-regulating USP18. *Alcohol Clin Exp Res* 40: 2329–2338. <https://doi.org/10.1111/acer.13226>.
23. Shi HX, Yang K, Liu X, Liu XY, Wei B, Shan YF, Zhu LH, Wang C. 2010. Positive regulation of interferon regulatory factor 3 activation by Herc5 via ISG15 modification. *Mol Cell Biol* 30:2424–2436. <https://doi.org/10.1128/MCB.01466-09>.
 24. Zhao C. 2016. Influenza B virus non-structural protein 1 counteracts ISG15 antiviral activity by sequestering ISGylated viral proteins. *Nat Commun* 7:12754. <https://doi.org/10.1038/ncomms12754>.
 25. Akutsu M, Ye Y, Virdee S, Chin JW, Komander D. 2011. Molecular basis for ubiquitin and ISG15 cross-reactivity in viral ovarian tumor domains. *Proc Natl Acad Sci U S A* 108:2228–2233. <https://doi.org/10.1073/pnas.1015287108>.
 26. Welch SR, Scholte FEM, Flint M, Chatterjee P, Nichol ST, Bergeron É, Spiropoulou CF. 2017. Identification of 2'-deoxy-2'-fluorocytidine as a potent inhibitor of Crimean-Congo hemorrhagic fever virus replication using a recombinant fluorescent reporter virus. *Antiviral Res* 147:91–99. <https://doi.org/10.1016/j.antiviral.2017.10.008>.
 27. Habjan M, Penski N, Spiegel M, Weber F. 2008. T7 RNA polymerase-dependent and -independent systems for cDNA-based rescue of Rift Valley fever virus. *J Gen Virol* 89:2157–2166. <https://doi.org/10.1099/vir.0.2008/002097-0>.
 28. Zhang W, Bailey-Elkin BA, Knaap RCM, Khare B, Dalebout TJ, Johnson GG, van Kasteren PB, McLeish NJ, Gu J, He W, Kikkert M, Mark BL, Sidhu SS. 2017. Potent and selective inhibition of pathogenic viruses by engineered ubiquitin variants. *PLoS Pathog* 13:e1006372. <https://doi.org/10.1371/journal.ppat.1006372>.
 29. Spengler JR, Patel JR, Chakrabarti AK, Zivcec M, García-Sastre A, Spiropoulou CF, Bergeron É. 2015. RIG-I mediates an antiviral response to Crimean-Congo hemorrhagic fever virus. *J Virol* 89:10219–10229. <https://doi.org/10.1128/JVI.01643-15>.
 30. Capodagli GC, McKercher MA, Baker EA, Masters EM, Brunzelle JS, Pegan SD. 2011. Structural analysis of a viral ovarian tumor domain protease from the Crimean-Congo hemorrhagic fever virus in complex with covalently bonded ubiquitin. *J Virol* 85:3621–3630. <https://doi.org/10.1128/JVI.02496-10>.
 31. James TW, Frias-Staheli N, Bacik J-P, Levingston Macleod JM, Khajehpour M, Garcia-Sastre A, Mark BL. 2011. Structural basis for the removal of ubiquitin and interferon-stimulated gene 15 by a viral ovarian tumor domain-containing protease. *Proc Natl Acad Sci U S A* 108:2222–2227. <https://doi.org/10.1073/pnas.1013388108>.
 32. Macleod JML, Marmor H, Garcia-Sastre A, Frias-Staheli N. 2015. Mapping of the interaction domains of the Crimean-Congo hemorrhagic fever virus nucleocapsid protein. *J Gen Virol* 96:524–537. <https://doi.org/10.1099/vir.0.071332-0>.
 33. Lindner HA, Fotouhi-Ardakani N, Lytvyn V, Lachance P, Sulea T, Menard R. 2005. The papain-like protease from the severe acute respiratory syndrome coronavirus is a deubiquitinating enzyme. *J Virol* 79: 15199–15208. <https://doi.org/10.1128/JVI.79.24.15199-15208.2005>.
 34. Capodagli GC, Deaton MK, Baker EA, Lumpkin RJ, Pegan SD. 2013. Diversity of ubiquitin and ISG15 specificity among nairoviruses' viral ovarian tumor domain proteases. *J Virol* 87:3815–3827. <https://doi.org/10.1128/JVI.03252-12>.
 35. Dzimianski JV, Beldon BS, Daczkowski CM, Goodwin OY, Scholte FEM, Bergeron É, Pegan SD. 2019. Probing the impact of nairovirus genomic diversity on viral ovarian tumor domain protease (vOTU) structure and deubiquitinase activity. *PLoS Pathog* 15:e1007515. <https://doi.org/10.1371/journal.ppat.1007515>.
 36. Bowick GC, Airo AM, Bente DA. 2012. Expression of interferon-induced antiviral genes is delayed in a STAT1 knockout mouse model of Crimean-Congo hemorrhagic fever. *Virol J* 9:122. <https://doi.org/10.1186/1743-422X-9-122>.
 37. Bente DA, Alimonti JB, Shieh W-J, Camus G, Stroher U, Zaki S, Jones SM. 2010. Pathogenesis and immune response of Crimean-Congo hemorrhagic fever virus in a STAT-1 knockout mouse model. *J Virol* 84: 11089–11100. <https://doi.org/10.1128/JVI.01383-10>.
 38. National Research Council of the National Academies. 2011. *Guide for the Care and Use of Laboratory Animals*, 8th ed. National Academy Press, Washington, DC.
 39. Bergeron É, Zivcec M, Chakrabarti AK, Nichol ST, Albariño CG, Spiropoulou CF. 2015. Recovery of recombinant Crimean Congo Hemorrhagic fever virus reveals a function for non-structural glycoproteins cleavage by furin. *PLoS Pathog* 11:e1004879. <https://doi.org/10.1371/journal.ppat.1004879>.
 40. Welch SR, Guerrero LW, Chakrabarti AK, McMullan LK, Flint M, Bluemling GR, Painter GR, Nichol ST, Spiropoulou CF, Albariño CG. 2016. Lassa and Ebola virus inhibitors identified using minigenome and recombinant virus reporter systems. *Antiviral Res* 136:9–18. <https://doi.org/10.1016/j.antiviral.2016.10.007>.
 41. Zivcec M, Metcalfe MG, Albariño CG, Guerrero LW, Pegan SD, Spiropoulou CF, Bergeron É. 1 December 2015, posting date. Assessment of inhibitors of pathogenic Crimean-Congo hemorrhagic fever virus strains using virus-like particles. *PLoS Negl Trop Dis* <https://doi.org/10.1371/journal.pntd.0004259>.